Society For Biomaterials

Preparation of poly(L-lactic acid)-modified polypropylene mesh and its antiadhesion in experimental abdominal wall defect repair

Zhigang Zhang,[1,2,3] Tianzhu Zhang,[1,3] Junsheng Li,[2] Zhenling Ji,[2] Hemei Zhou,[2] Xuefeng Zhou,[1,3] Ning Gu[1,3]

[1]Jiangsu Key Laboratory for Biomaterials and Devices, State Key Laboratory of Bioelectronics, School of Biological Science and Medical Engineering, Southeast University, Sipailou 2, Nanjing 210096, China
[2]Department of General Surgery, Affiliated Zhong-Da Hospital, Southeast University, Dingjiaqiao 87, Nanjing 210009, China
[3]Suzhou Key Lab of Biomedical Materials and Technology, Research Institute of Southeast University in Suzhou, Ren Ai Road 150, Suzhou Industrial Park, Suzhou 215123, China

Received 19 October 2012; revised 22 February 2013; accepted 25 February 2013
Published online 00 Month 2013 in Wiley Online Library (wileyonlinelibrary.com). DOI: 10.1002/jbm.b.32947

Abstract: A new type of polypropylene (PP) hernia mesh, modified with poly(L-lactic acid) (PLLA), was developed and used to repair rat abdominal wall defect. The PP mesh was first treated with oxygen plasma and then grafted with PLLA in phosphorus pentachloride (PCl_5) solution in dichloride methane. The water contact angle changed during the procedure, and the coverage percentage of PLLA on the PP was about 80%. ATR-FTIR spectroscopy measurements showed the existence of carbonyl group absorption peak (1756.9 cm^{-1}), and atomic force microscope and scanning electron microscope morphological observation indicated that the surface of the PP mesh was covered with PLLA graft. X-ray photoelectron spectroscopy spectra was used to probe chemical group changes and confirmed that the PLLA was grafted onto the PP. A total of 36 Sprague–Dawley rats were randomly divided into six groups, and they received either modified meshes (experimental groups) or PP meshes (control groups) to repair abdominal wall defects. All animals survived until the end of the experiment. Rats in each group were dissected after the operation (after 1 week, 2 weeks, and 1 month, respectively), and the adhesion effects were evaluated. Sections of the mesh parietal peritoneum overlap were examined histologically and graded for inflammation reaction. Compared with the control groups, the experimental groups showed a better ability to resist peritoneal cavity adhesions ($P < 0.05$), and there was no increase in inflammation formation ($P > 0.05$). This new type of PLLA-modified PP mesh displayed an additional property of antiadhesion in animal abdominal wall defect repair. © 2013 Wiley Periodicals, Inc. J Biomed Mater Res Part B: Appl Biomater 00B: 000–000, 2013.

Key Words: polypropylene, poly(L-lactic acid), hernia repair, mesh, antiadhesion

How to cite this article: Zhang Z, Zhang T, Li J, Ji Z, Zhou H, Zhou X, Gu N. 2013. Preparation of poly(L-lactic acid)-modified polypropylene mesh and its antiadhesion in experimental abdominal wall defect repair. J Biomed Mater Res Part B 2013:00: 000–000.

INTRODUCTION

One of the most important prosthetic materials, polypropylene (PP), is widely used in medicine, especially for hernia repair, because of its highly physiochemical performance, such as flexibility, nice chemical stability, and reduced foreign body reaction.[1] However, the PP mesh needs to be separated from the viscus during hernia repair, which could cause bowel adhesion formation, bowel rupture, and other serious complications postoperatively.[2–4] The complications, to some extent, were caused by foreign body reactions of material. PP was nonabsorbable and nondegradable polymeric material with an acceptable biocompatibility. Polyester (PET) as an alternative to PP hernia repair was widely used in clinical because of its hydrophilic and biodegradable properties. But the long-term complications (infection, fistula, and recurrence) were the disadvantages of PET. Furthermore, PP as a nonabsorbable material was much more stable or stronger than PET used as hernia repair; therefore, most of the new mesh was composed of PP.[5,6] The great demand in the medicine market for antiadhesion PP meshes has accelerated the development of PP mesh modification procedures. Over several decades, various methods have been used to modify the surface of PP or polyethylene to improve its surface properties, such as plasma treatment, corona discharge, and photoinitiated grafting.[7]

Cold plasma is one of the convenient and efficient methods to modify the surfaces of polymers.[8,9] After treatment by cold plasma, the bulk properties of polymeric material do not change, because this modification procedure is limited to the outermost layers of several hundred angstroms. Meanwhile, the activated surface of the polymer could be

Correspondence to: T. Zhang (e-mail: zhangtianzhuglq@sina.com), L. Zhen (e-mail: zlji@vip.sina.com) or N. Gu (e-mail: guning@seu.edu.cn)

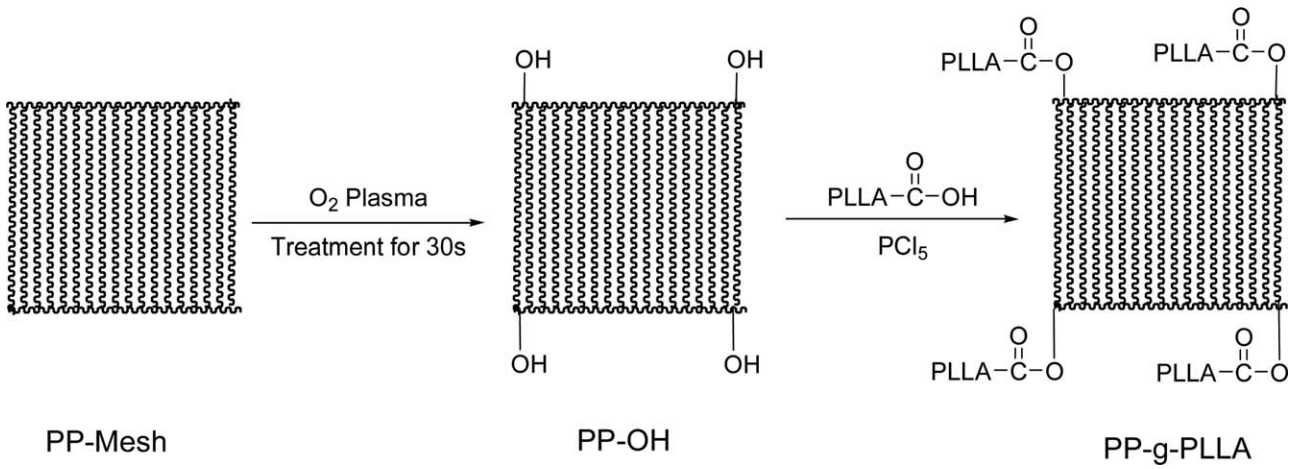

SCHEME 1. Schematic illustration of grafting poly(L-lactic acid) (PLLA) on hydroxyl-terminated polypropylene (PP-OH) surface.

grafted by some useful and selected elements or specific functional groups, such as glycidyl methacrylate, acrylic acid, α-ally glycoside, or heparin.[10–14]

To the best of our knowledge, poly(lactic acid) (PLA) is the most extensively researched and used biodegradable and renewable PET. Biocompatibility and nontoxic degradation properties make the PLA a natural choice for biomedical applications.[15]

In the past, grafting poly(L-lactic acid) (PLLA) onto hydroxyl-terminated substrate was accomplished through ring-opening polymerization. Herein, with oxygen plasma–oxidized PP mesh (PP-OH) as the co-initiator, we grafted PLLA onto the oxygen plasma functionalized surface of PP (PP-OH) in the presence of PCl_5. Water contact angle (WCA) was used to measure surface energy change. The chemical structure of surface was observed by the attenuated total reflectance Fourier transform infrared (ATR-FTIR) spectra, and the topographies of surface was characterized by scanning electron microscope (SEM), atomic force microscope (AFM), and x-ray photoelectron spectroscopy (XPS) spectra. These meshes were also used in the repair of rat abdominal wall defects to check for antiadhesion properties.

EXPERIMENTAL SECTION

Preparation of modified mesh

Materials. The PLLA (M_W = 300,000) was purchased from Shandong Institute of Medical Instruments (Shandong, China). PP mesh was obtained from "X" company. Native PP meshes, about 1.5 cm^2 in size, were tailored. Dichloride methane (CH_2Cl_2) and phosphorus pentachloride (PCl_5) were purchased from Wanqing Chemical Company. Dichloride methane (CH_2Cl_2) was dried with CaH_2, and PCl_5 was used as received.

Oxidation of PP mesh. PP mesh samples were first extracted with CH_2Cl_2 for 24 h to remove any additional antioxidants and other soluble additives. After being dried under vacuum, they were treated in oxygen plasma equipment for 30 s (PDC-M, intensity = 40 W, oxygen flow = 800 mL/min). Then, the PP meshes were washed with CH_2Cl_2 and dried under vacuum again. After this procedure, a hydroxylated PP mesh sample was obtained, and designated PP-OH.

Graft polymerization of PLLA onto PP mesh surface. First, 0.1000 g PLLA (M_W = 300,000) was sufficiently dissolved in 5 mL dried CH_2Cl_2 in a round flask, and then 0.0070 g PCl_5 (molar ratio of PLLA to PCl_5 = 1:100) was added. One hour later, the PP-OH mesh samples were immersed into the prepared solution in the flask for 2 h under N_2 atmosphere. After 2 h, the PP mesh sample was removed from the flask, washed twice with CH_2Cl_2, and dried at 60°C. These PP meshes were designated PP-g-PLLA meshes (Scheme 1).

Characterization of PP mesh and PP flake. To observe the chemical structures and the morphologies of the surface at different experimental stages conveniently, we used two forms of PP (mesh and flake) during the entire experiment. Using a molten method, native PP mesh changes its form to flakes.

The sessile drop method was used for contact angle measurements, at 20 ± 1.5°C, using a commercial contact angle meter (Solon Tech, Shanghai, China). The diameter of the droplet used for the measurement was about 2 mm. Ultrapure water droplets were placed at six different positions on each sample, and the average value was obtained. The experimental error of the measurements was about ±2°.

The ATR-FTIR spectra of the PP meshes were obtained using a Mattson Galaxy 4201 spectrometer with a Wilks model 10 ATR accessory at an angle of 45°, using a KRS-5 crystal. The spectra, which were the sum of 256 individual scans, were recorded at 4 cm^{-1} resolution, between 4000 and 400 cm^{-1}.

The surfaces of the PP flake were probed by AFM (Agilent PicoPlus). The surface topographies of the PP meshes were detected by SEM.

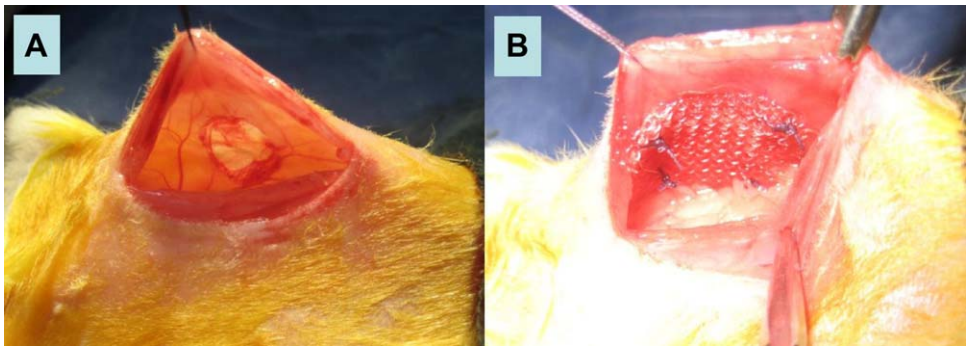

FIGURE 1. (A) Full-thickness defect of the abdominal wall was created. (B) The abdominal wall defect was repaired with the mesh using the intraperitoneal underlay technique. [Color figure can be viewed in the online issue, which is available at www.interscience.wiley.com.]

XPS (Thermo ESCALAB 250) was used to determine the surface composition of the PP flakes. A monochromatic Al Kα x-ray source was operated at 1486.6 eV, and the anode x-ray source was operated at 15 kV and 8.9 mA. Survey spectra were acquired from 0 to 1200 eV binding energy (BE), with a pass energy of 160 eV, a step size of 1.0 eV, and a dwell time of 50 min. For high-resolution spectra, a pass energy of 17.9 eV, an energy step of 0.1 eV, and a dwell time of 1.2 s were used, with a typical average of 12 scans. The operating pressure of the spectrometer was $\sim 10^{-9}$ mbar. All data were collected and analyzed using the software provided by the manufacturer.

Animal application of PP mesh

Animals and groups. The study was performed in compliance with the health system experimental animal management provisional regulations of China. A total of 36 female Sprague–Dawley rats, weighing 250–300 g each, were randomly divided into six groups of six animals each. Groups 1–3 were the experimental groups, and groups 4–6 were the control groups. All of the rats were housed in the laboratory for 1 week before the study, under standard conditions (temperature: 22°C, humidity: 30%) and fed standard laboratory food and tap water *ad libitum*.

Surgical procedure. The 36 rats were anaesthetized by intraperitoneal injection of 3% isoamyl benzene of pentobarbital sodium (60 mg/kg bw). The abdomen was shaved and disinfected with 0.5% povidone–iodine, and a 3-cm median incision was made. A full-thickness defect, 1 cm in diameter, was created at the lower right abdominal wall, consisting of fascia, muscle, and peritoneum [Figure 1(A)]. Both types of meshes were sterilized by ethylene oxide. The abdominal wall defects of groups 1–3 and groups 4–6 were repaired with the PP-g-PLLA meshes and PP meshes, respectively, using intraperitoneal underlay technique [Figure 1(B)]. The meshes were fixed to the peritoneum with four interrupted Vicryl 4-0 sutures. The omenta were put to the left abdominal cavity to make the visceral surface of the mesh contact the bowels directly. Then, the muscle layer and skin incisions were closed with a continued Vicryl 4-0 suture. Postoperatively, all the animals were housed in individual cages, with water provided continuously; feed was restricted for 6 h.

Macroscopic and microscopic evaluations. After the repair, each group of rats was dissected at different time points, as follows: groups 1 and 4, 1 week; groups 2 and 5, 2 weeks; and groups 3 and 6, 1 month. After receiving the same anaesthetic protocol, a U-shaped skin incision was made to observe the adhesions. The adhesions were graded according to an adhesion scoring system (Table I).[16,17] Sections of the mesh parietal peritoneum overlap were examined histologically and graded for inflammation, using a semiquantitative scoring system (no inflammation = 0; giant cells, lymphocytes, plasma cells = 1; giant cells, plasma cells, eosinophils, neutrophils = 2; many inflammatory cells, microabscess = 3).[18] All animals were euthanized by cervical dislocation. The adhesions and inflammation were scored, and the adhesion regions were excised for histopathological examination.

Statistical analysis

The SPSS 13.0 for Windows program was used for data analysis. Statistical significance was determined by a two-tailed Student's t test. Significance was assumed at a value of $P < 0.05$.

RESULTS

WCA

For the PP flake, the WCA was 95.0°. After the treatment of oxygen plasma, the WCA of the PP-OH flake was 65.7°. After grafting with PLLA, the WCA of the PP flake was 87.0°.

TABLE I. Adhesion Grading Scale

Score	Extent of Adhesions (%)	Tenacity and Severity of Adhesions
0	0	No adhesions
1	≤25	Gentle blunt dissection required to free adhesions
2	25–50	Aggressive blunt dissection required to free adhesions
3	>50	Sharp dissection required to free adhesions

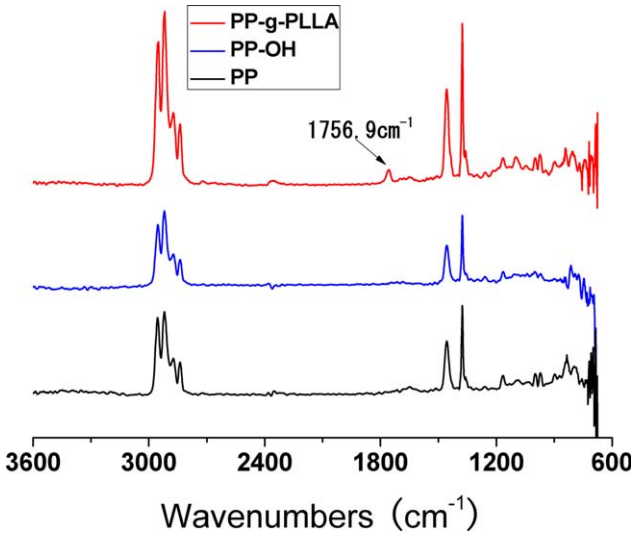

FIGURE 2. The comparisons of ATR-FTIR spectra of PP mesh, PP-OH mesh, and PP-g-PLLA mesh. [Color figure can be viewed in the online issue, which is available at www.interscience.wiley.com.].

ATR-FTIR spectrum

After the oxidation of oxygen plasma, the PP-OH flake showed no more obvious absorption peak than the native PP flake. Compared with both native PP flake and PP-OH flake, PP-g-PLLA flake showed a new absorption peak (1756.9 cm^{-1}; Figure 2).

AFM and SEM observation

Atomic force microscopy observations indicated that most of the surfaces of the PP flakes were nearly smooth, except for some apparent spherulites. The diameter of these visible spherulitic crystallines ranged 1–17 μm in the AFM micrographs [Figure 3(A)]. After the oxidation of the oxygen plasma, the surfaces of the PP flakes became slightly rough, as can be seen in the AFM images in Figure 3(B). Some of the apparent spherulites that had been observed in the native PP flakes were destroyed. At the same time, many small spherulites, dispersed all over the PP flake surfaces, and ranging 0.2–0.7 μm, were detected. After being grafted with PLLA, the surfaces of the PP-g-PLLA flakes were rougher than those of the PP-OH flakes [Figure 3(C)], and they became thicker and softer.

There are no apparent differences among the three stages of PP mesh in low magnification [Figure 4(A1,B1,C1)]. Under high magnification, SEM micrographs showed that there were some regular and slight striations along the longitudinal axis of the monofilament of PP mesh, and the PP mesh (PP-OH) surface became unsmooth after being treated with the oxygen plasma for 30 s, and that the sizes of the surface ridges ranged 0.2–0.6 μm [Figure 4(B2)]. The morphology changes of the PLLA-grafted PP mesh surface were much more obvious than those of both the unprocessed PP mesh and the oxygen plasma–oxidized PP mesh.

Chemical changes probed by XPS

The native PP mesh was probed using XPS chemical analysis, and the results showed the oxygen 1s (O_{1s}) spectra of native PP mesh with a peak at the BE of 531.6 and 532.1 eV, with count around 4180.8–4193.1 (Figure 5). The carbon 1s (C_{1s}) peak at the BE of around 284.7 eV (Figure 6).

After being treated with oxygen plasma for 30 s, the O_{1s} XPS spectra of peak at the BE of around 532.3 eV and the count is 78655.1 (Figure 7). The C_{1s} core-level spectrum can be curve-fitted with four peak components having BEs at about 288.2, 287.4, 286.2, and 284.7 eV (Figure 8).

After grafting PLLA onto the PP mesh, we obtained two O_{1s} XPS spectra peaks (533.7 and 532.3 eV) (Figure 9). The C_{1s} core-level spectrum can be curve-fitted with four peak components having BEs at about 289.1, 287.1, 285.8, and 284.7 eV (Figure 10).

Adhesion and inflammation

All of the animals in the study survived until the respective end points (control groups—dead: 0 case; infection: four

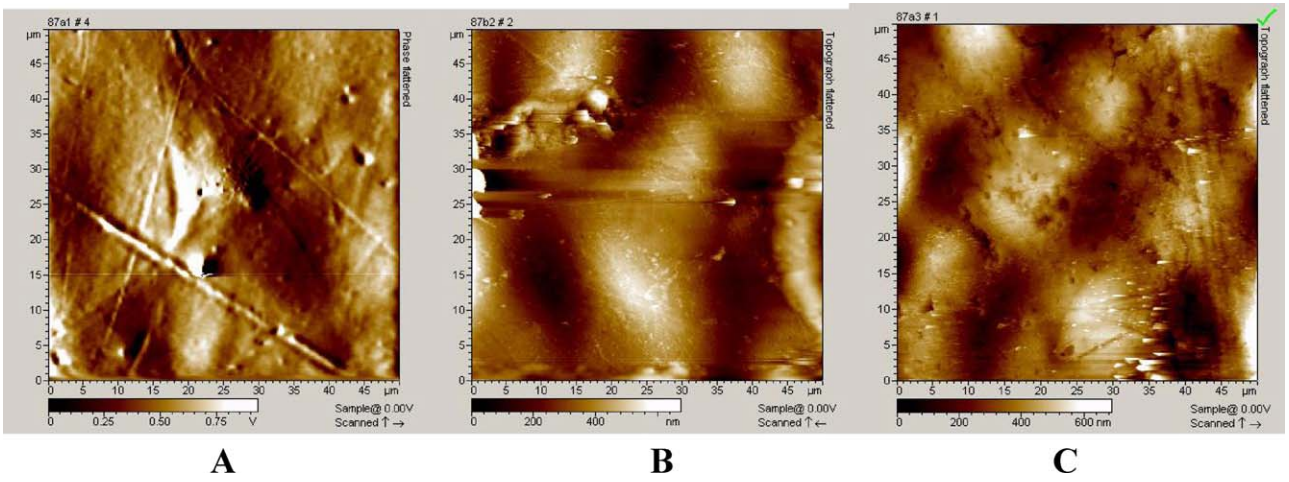

FIGURE 3. AFM micrographs of PP flakes (A), PP-OH flakes (B), and PP-g-PLLA flakes (C). [Color figure can be viewed in the online issue, which is available at www.interscience.wiley.com.].

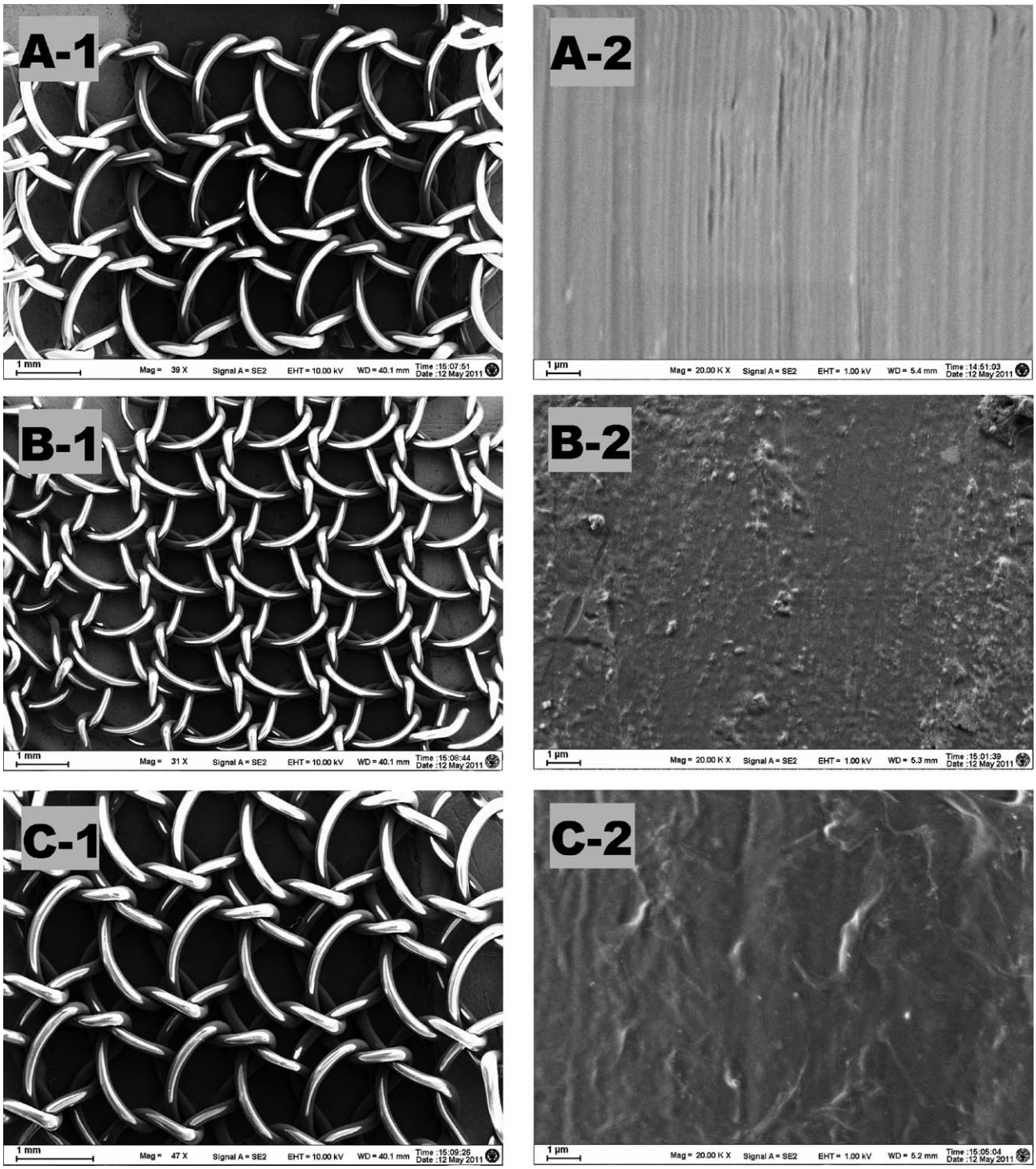

FIGURE 4. (A1, A2) Aspect of the PP mesh surface observed through SEM. (B1, B2) Aspect of the PP mesh (PP-OH) surface (oxidized with oxygen plasma for 30 s) observed through SEM. (C1, C2) Aspect of the PP-g-PLLA mesh surface observed through SEM.

cases; abscess: two cases; experimental groups—dead: 0 case; infection: 0 cases; abscess: 0 cases). The adhesion scores for each group at the different postoperative time points are provided in Table II. By comparing the adhesion scores, as shown in Figure 11, the experimental groups were superior to control groups. At different observation time points, we gained corresponding different images (Figures 12 and 13). The serious inflammation reactions of control groups were observed as in Figure 14.

DISCUSSION

Hydrophilicity study

We used the pressing molten method to prepare the PP flakes for the WCA measurements, which were treated co-

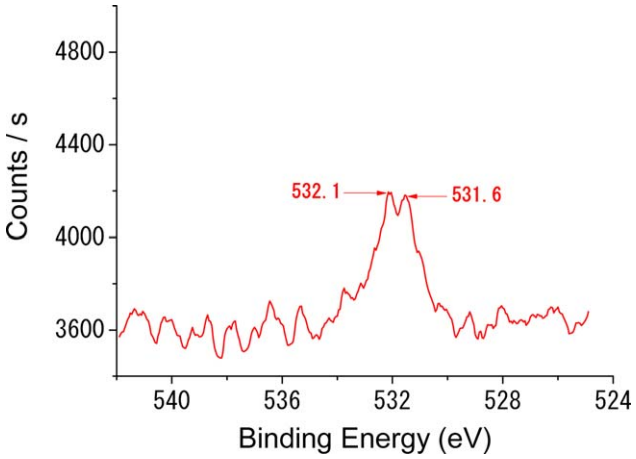

FIGURE 5. O_{1s} XPS spectra of native PP mesh. [Color figure can be viewed in the online issue, which is available at www.interscience.wiley.com.].

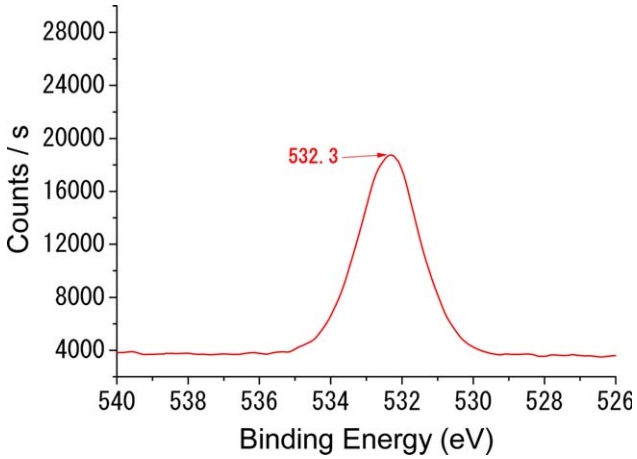

FIGURE 7. O_{1s} XPS spectra of PP-OH mesh. [Color figure can be viewed in the online issue, which is available at www.interscience.wiley.com.].

instantaneously; this method was the same for the experimental PP mesh. The WCA of the PP flake changed according to the treatment procedure. The PP flake with a hydrophobic WCA of **(**95.0°**)** showed that the surface of the PP was hydrophobic. After the oxidation of oxygen plasma, the formed hydroxyl group on the PP surface resulted in slight hydrophilicity, with a contact angle of 65.7°; further grafting polymerization of PLLA on the PP surface recovered the WCA to 87.0°. The surface of the PLLA-grafted PP flake was hydrophobic, whereas the WCA of the pure PLLA smooth film was 77°.[19,20] These two measured WCA seem paradoxical; a theoretical calculation might help interpret this phenomenon. The relationship between the contact angle of a flat surface, θ, and that of a suitably rough surface, θ_r, can be expressed by Eq. ((1))[21,22]:

$$\cos\theta_r = f_1\cos\theta - f_2 \quad (1)$$

where f_1 and f_2 are the fractional interfacial areas of the smooth PPLA film and of the air in the PLLA-grafted PP flake, respectively, and $f_1 + f_2 = 1$. From Eq. ((1)), f_1 can be calculated according to the values of θ_r and θ. Here, $\theta_r = 87.0°$ and $\theta = 77°$; therefore, $f_1 = 0.8$. The calculation result indicates that the coverage percentage of PLLA on PP flake is approximately 80%.

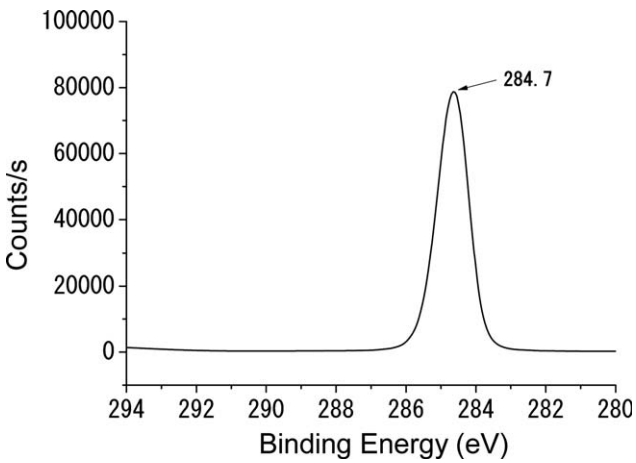

FIGURE 6. C_{1s} XPS spectra of native PP mesh.

ATR-FTIR spectrum morphologies of PP mesh

There were no obvious changes between PP and PP-OH in the ATR-FTIR spectra. However, after treating them with oxygen plasma and grafting with PLLA, a new emerging absorption peak, around 1756.9 cm^{-1}, could be detected in the spectrum, indicating that the new absorption peak was related to the carbonyl (C═O) of the PLLA graft ester groups (Figure 2).

AFM and SEM observation of PP flakes

The surfaces of the PP flakes were nearly smooth, but some apparent spherulitic crystallines (diameter, range 1–17 μm) have also been observed in the AFM micrographs [Figure 3(A)]. As we known, molten method was used to prepare

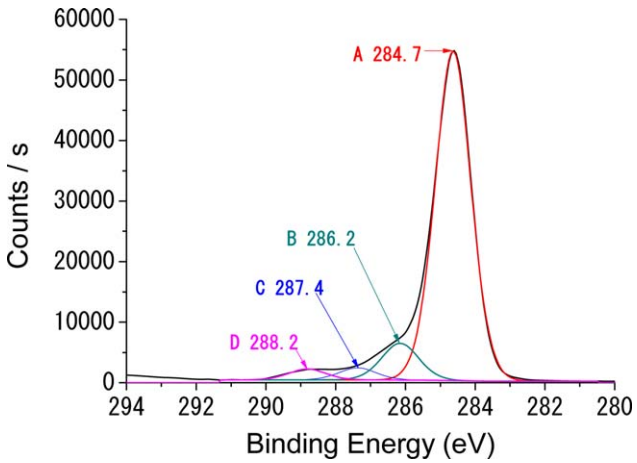

FIGURE 8. C_{1s} XPS spectra of PP-OH mesh. [Color figure can be viewed in the online issue, which is available at www.interscience.wiley.com.].

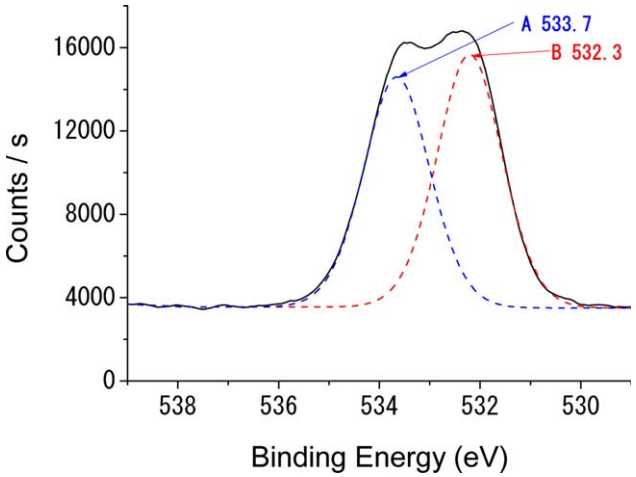

FIGURE 9. O_{1s} XPS spectra of PP-g-PLLA mesh. [Color figure can be viewed in the online issue, which is available at www.interscience.wiley.com.].

the PP flakes, which could form small crystallines. After treatment with oxygen plasma for 30 s, most of the apparent spherulites of PP flakes were destroyed and many small spherulites were dispersed all over the PP flake surfaces. Observed through AFM images, their diameters ranged 0.2–0.7 μm. Therefore, the surfaces of the PP-OH flakes became slightly rough (Figure 3). Furthermore, the surface of the final grafted samples (PP-g-PLLA flakes) was rougher (look like dispersed rugosity) than those of the PP-OH flakes, which could help us to distinguish them from the untreated PP flakes.

To observe the surface change of PP mesh directly, we chose PP mesh as the samples to be checked by SEM. It is known that the surface of the monofilament of the native PP mesh is smooth. But under high magnification, SEM micrographs although showed that there were some regular and slight striations along the longitudinal axis of the monofilament of PP mesh, because of its drawing-off extrusion process of production [Figure 4(A2)]. The surface changes of PP-OH, which we observed from AFM, were also detected from SEM and displayed as unsmooth surfaces and the surface ridges ranged 0.2–0.6 μm [Figure 4(B2)]. Compared with the changes of the surfaces among PP-g-PLLA, PP-OH and PP, the surface of PP-g-PLLA were the most rough. Both AFM and SEM morphology changes could indicate that the PP mesh surface was covered with a thick or wavelike material [Figures 3 and 4(C2)].

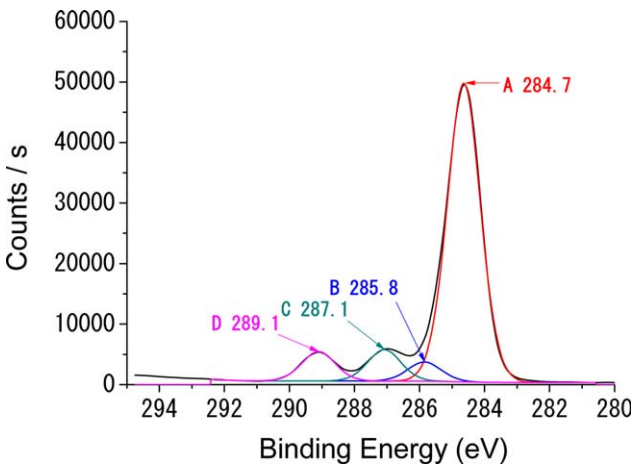

FIGURE 10. C_{1s} XPS spectra of PP-g-PLLA mesh. [Color figure can be viewed in the online issue, which is available at www.interscience.wiley.com.].

Surface analysis by XPS

The XPS results showed the O_{1s} spectra of native PP mesh with a peak at the BE of 531.6 and 532.1 eV, but with the extremely low count of only around 4180.8–4193.1. Actually, the native PP mesh has no oxygen element, and most of the chemical elements are carbon and hydrogen. The detected O_{1s} peak with the extremely low count indicates that O probably is the external impurity. Furthermore, the carbon 1s (C_{1s}) peak at the BE of around 284.7 eV should correspond to C—C/C—H species (Figures 5 and 6).

The O_{1s} XPS spectra of peak of the oxidized PP flakes (PP-OH) at the BE of around 532.3 eV corresponded to oxygen atoms bonding to hydrogen (C—O—H bonds), and the count is 78655.1, much higher than that of the native PP (Figure 7). The C_{1s} core-level spectrum of PP-OH can be curve-fitted with four peak components having BEs at about 288.2, 287.4, 286.2, and 284.7 eV. The C_{1s} peak at a BE of around 284.7 eV corresponds to C—C/C—H species. The peak components at the BEs of about 288.2, 287.4, and 286.2 eV are attributed to the >C═O, —C—O—, and —CH_2OH species, respectively (Figure 8).[23] Oxygen plasma is a well-known surface-modifying technique that aims to remove surface contaminants and decrease energy of the interfacial molecules. After being treated with oxygen plasma, in theory, the PP mesh got the oxygen element, which was denoted PP-OH mesh. Through analyzing the C1s

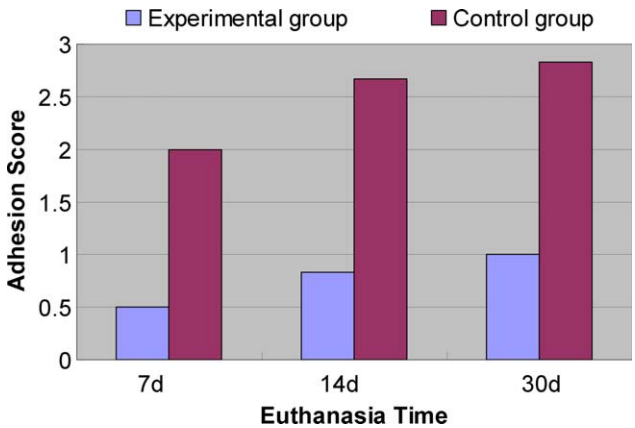

FIGURE 11. Histogram of the means of adhesion scores in Table II. At different postoperative euthanasia times, the tendency of the adhesion scores of each group increased constantly over time. The adhesion scores of the experimental group were obviously lower than those of the control group. [Color figure can be viewed in the online issue, which is available at www.interscience.wiley.com.].

FIGURE 12. (A) Seven days after defect repair procedure with PP-g-PLLA mesh. The visceral surface of the mesh was smooth and without any adhesion formation. Adhesion score was 0. (B) Fourteen days after defect repair procedure with PP-g-PLLA mesh. There were a few slender fibrous and omental adhesions, and most were formed at the edges of the mesh. The rest of the mesh visceral surface was smooth. Adhesion score was 1. (C) Thirty days after defect repair procedure with PP-g-PLLA mesh. The degrees of adhesion were the same as (B). Adhesion score was 1. [Color figure can be viewed in the online issue, which is available at www.interscience.wiley.com.].

XPS spectra, we deduced that there were four structures of C species outside of the PP-OH mesh.

Through XPS analysis of PP-g-PLLA, we obtained two O_{1s} XPS spectra peaks (Figure 9). The 533.7 eV peak corresponds to —C—O— species, and the 532.3 eV peak corresponds to C═O species. The C_{1s} core-level spectrum can be curve-fitted with four peak components having BEs at about 289.1, 287.1, 285.8, and 284.7 eV. The C_{1s} peaks at a BE of around 284.7 eV corresponds to C—C/C—H species, and other peak components at the BEs of 289.1, 287.1, and 285.8 eV are attributed to —O—C═O, —C—O—, and —CH—OH species, respectively (Figure 10).[24,25] As we know, after the PP mesh was modified by PLLA, which was designated PP-g-PLLA, its chemical structures had the conservative characteristics of each polymer material. The XPS spectra BE analysis showed that PP-g-PLLA had two types of oxygen element and four types of carbon species.

Native PP, PP-OH, and PP-g-PLLA showed different features at each modified step. During the chemical modification period, the surface energy and chemical structure of PP changed. Through WCA observation, PP became hydrophilic after being treated with oxygen plasma for 30 s, and it recovered its hydrophobic property. Although both PP and PLLA are hydrophobic, there is a question of how PLLA was able to recover the hydrophobic property of PP-OH and how it was performed. This phenomenon might be explained by the reaction of PLLA to the PP-OH hydroxyl group. We used the WCA in Eq. ((1)) to calculate the coverage percentage of PLLA on PP, and the result was about 80%.

The ATR-FTIR spectra showed that PP-g-PLLA had a new absorption peak (1756.9 cm^{-1}), which was related to the carbonyl (C═O) and was different from PP and PP-OH. It is well known that PLLA has ester groups; therefore, we believe that the 1756.9 cm^{-1} peak of PP-g-PLLA was endued by PLLA. We did not obviously detect the hydroxyl group absorption peak of PP-OH, but the WCA and XPS spectra demonstrated that the hydroxyl groups were indeed on the PP-OH.

AFM and SEM results showed that after being treated by oxygen plasma for 30 s, the surface of PP was slightly destroyed, but the entire monofilament was not impaired, leading us to believe that the oxygen plasma was moderate and only modified the outermost part of the PP. Both the AFM and SEM images showed that there were some structures on the PP, which we believed was the PLLA graft.

The XPS spectra probed each step of the PP modification procedure and identified the chemical group changes taking place on the PP. Oxygen plasma treatment gave the hydroxyl

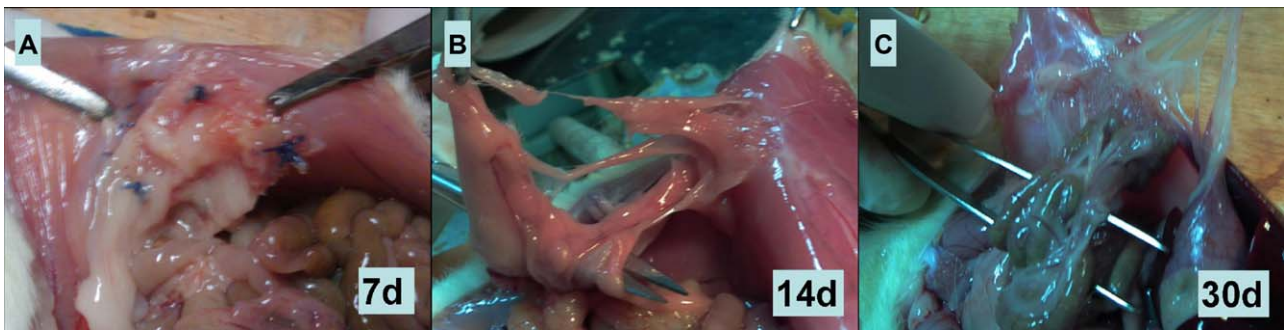

FIGURE 13. (A) Seven days after defect repair procedure with PP mesh. Nearly, the entire visceral surface of the mesh was covered with thick omental adhesions. Adhesion score was 3. (B) Fourteen days after defect repair procedure with PP mesh. The entire mesh was covered with adhesion. Adhesion score was 3. (C) Thirty days after defect repair procedure with PP mesh. Serious adhesions formed on the visceral surfaces, consisting mostly of small bowel loops and part of the omentum. Adhesion score was 3. [Color figure can be viewed in the online issue, which is available at www.interscience.wiley.com.].

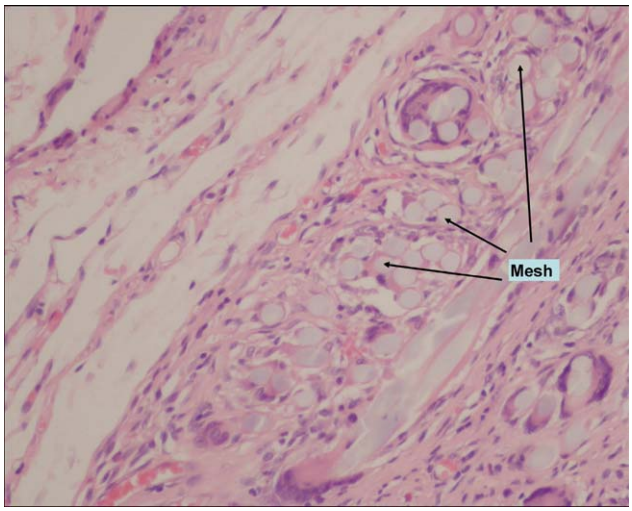

FIGURE 14. Microscopically examined mesh parietal peritoneum overlap (magnification ×40). Inflammation score was 2. [Color figure can be viewed in the online issue, which is available at www.interscience.wiley.com.].

groups to PP, and PLLA reacted with the hydroxyl groups; those results were found and confirmed by the O_{1s} and C_{1s} XPS spectra. Therefore, we confidently believed that PP-g-PLLA was the result of PLLA grafting onto PP.

Evaluations and comparisons of adhesion and inflammation

Fortunately, all the rats in the study survived until the respective end points. Through dissection of animals, the adhesions of experimental groups were smaller and slighter than the ones of control groups. Nearly, all the adhesions of control groups needed sharp or aggressive blunt dissection to free, whereas the ones of experimental groups were easy to free. The formers always resulted in omenta tearing or bowels rupture (control groups—dead: 0 case; infection: four cases; abscess: two cases; experimental groups—dead: 0 case; infection: 0 cases; abscess: 0 cases). Comparing Figure 12 with Figure 13, we conclude that the adhesions of the control groups were never freed by gentle blunt dissection, whereas the adhesions of the experimental groups were little or freed easily. Actually, the tenacity of adhesions was also scored and showed significant difference ($P < 0.05$) (Table II).

By comparing the adhesion scores, as shown in Figure 11, we directly observed that the experimental groups showed lower score means than the control groups during the entire observation period. The statistical analysis also indicated that at each observed time point, the adhesion extent scores of the experimental groups were significantly lower than those of the control groups ($P < 0.05$). Furthermore, after the gross anatomy, the adhesions of the experimental groups seemed to be much slighter, and most were prone to being located at the edges of the meshes. The adhesions of the experimental groups always consisted of omenta and fibrous belts. However, the adhesion formations of the control groups showed widespread and serious (bowels were included) in most situations. The adhesions of the experimental groups were thinner and smoother than those of the control groups.

Figures 12 (experimental group) and 13 (control group) are the abdominal laparotomy images (mesh included) at different postoperative time points. Histological examinations to evaluate inflammation of the mesh parietal peritoneum overlap in each group at different postoperative times showed that the inflammation grades of both the experimental and control groups alleviated gradually, but there were no statistically significant differences ($P > 0.05$). The highest inflammation grade of control groups was 2 (Figure 14).

It has been clearly shown in literature that PP mesh leads to a high rate of adhesion formation with abdominal viscera, especially the small bowel.[2,26] A similar adhesion formation phenomenon was observed in this experiment. In the control groups, nearly the entire mesh surface was covered with adhesions, which consisted of thick omenta and small bowels. Meanwhile, the similar adhesion formations at the edges of the meshes were also observed in the control groups, but more serious. It is known that PP mesh is tough and tensile, and after the tailoring process to make the mesh pieces, the margins became ragged. Visceral organs, especially the bowels, omenta, and mesenteries, were first rubbed and hooked by the hard and ragged mesh margins, and then adhesions formed at the edges of the mesh. We

TABLE II. Scoring and Comparison of Adhesion, Fibrosis, and Inflammation Between the Experimental and Control Groups

Group	Extent of Adhesions (Mean ± SD)	Tenacity of Adhesions (Mean ± SD)	Inflammation Score (Mean ± SD)
Euthanasia at 7 days			
Experimental group ($n = 6$)	0.50 ± 0.55	0.17 ± 0.41	1.17 ± 0.75
Control group ($n = 6$)	2.00 ± 0.63	2.33 ± 0.52	1.67 ± 0.52
Statistical significance	$P = 0.001$	$P = 0.000$	$P = 0.209$
Euthanasia at 14 days			
Experimental group ($n = 6$)	0.83 ± 0.75	0.17 ± 0.41	1.00 ± 0.63
Control group ($n = 6$)	2.67 ± 0.82	2.50 ± 0.55	1.50 ± 0.55
Statistical significance	$P = 0.002$	$P = 0.000$	$P = 0.174$
Euthanasia at 30 days			
Experimental group ($n = 6$)	1.00 ± 0.63	0.33 ± 0.52	0.50 ± 0.55
Control group ($n = 6$)	2.83 ± 0.75	2.83 ± 0.41	0.67 ± 0.52
Statistical significance	$P = 0.001$	$P = 0.000$	$P = 0.599$

found that the Vicryl 4-0 sutures were absorbed about 14 days after the operations and had no more obvious influence on the adhesions.

PLLA is one of the most innovative materials being developed for a wide range of applications, because of such excellent and unique features as biodegradability, thermoplastic processability, and eco-friendliness.[26] Those applications range from commodity plastics and packaging to medicine surgery materials, pharmaceuticals, and other fields. PLLA, hyaluronic acid and carboxymethylcellulose have been well studied and used as adhesion barriers to prevent adhesions either in experimentations or clinical trials.[27,28] Therefore, the future of the application of PLLA in medicine, which rests on its biodegradability and biocompatibility of the degradation product with the human body will become more and more bright. In this study, it was evident that the ester groups were the key component groups of PLLA, and they were also obviously detected by ATR-FTIR spectroscopy. However, we could not observe the carbonyl (C═O) absorption peak of the PP-OH mesh. Therefore, we deemed that PLLA had been effectively grafted onto the surface of the PP-OH mesh by this method.

CONCLUSIONS

PLLA can be grafted onto the oxygen plasma–functionalized surface of PP mesh (PP-OH) with the aid of PCl_5. This finding was confirmed by WCA measurements, ATR-FTIR absorption peak (around 1756.9 cm^{-1}), AFM and SEM observations, and XPS spectra probe. Compared with the untreated PP mesh, PLLA-modified PP mesh (PP-g-PLLA) displayed a better performance in resisting abdominal cavity adhesions in an animal model of abdominal wall defect repair. However, there were no remarkable differences in inflammation grade between the native PP mesh and the PP-g-PLLA mesh. On the basis of these laboratory findings, PLLA-modified PP mesh may be considered an antiadhesion repair mesh after further improvements in the surface structure and properties.

ACKNOWLEDGEMENTS

The work is supported by the Ministry of Education of China Key Science and Technology Research Project (109072), Suzhou High-Tech Enterprise Innovation Fund (SG0921), National Important Science Research Program of China (2011CB933503), International cooperation program awarded by Ministry of Science and Technology of China (2008 DFA51180), National Natural Science Foundation of China (Nos. 50872021, 90406023), and Qing Lan Project.

REFERENCES

1. Cho DL, Shin KH, Lee WJ, Kim DH. Improvement of paint adhesion to a polypropylene bumper by plasma treatment. J Adhes Sci Technol 2001;15:653–664.
2. Bellón JM, Buján J, Contreras LA, Carrera-San MA, Jurado F. Comparison of a new type of polytetrafluoroethylene patch (Mycro Mesh) and polypropylene prosthesis (Marlex) for repair of abdominal wall defects. J Am Coll Surg 1996;183:11–18.
3. Lo DJ, Bilimoria KY, Pugh CM. Bowel complications after prolene hernia system (PHS) repair: A case report and review of the literature. Hernia 2008;12:437–440.
4. Goswami R, Babor M, Ojo A. Mesh erosion into caecum following laparoscopic repair of inguinal hernia (TAPP): A case report and literature review. J Laparoendosc Adv Surg Tech A 2007;17:669–672.
5. Klosterhalfen B, Klinge U, Hermanns B, Schumpelick V. Pathology of traditional surgical nets for hernia repair after long term implantation in humans. Chirurg 2000;71:43–51.
6. Leber GE, Garb JL, Alexander A, Reed WP. Long-term complications associated with prosthetic repair of incisional hernias. Arch Surg 1998;133:378–382.
7. Pandiyaraj KN, Selvarajan V, Deshmukh RR, Gao C. Modification of surface properties of polypropylene (PP) film using DC glow discharge air plasma. Appl Surf Sci 2009;255:3965–3971.
8. Liston EM. Plasma Surface Modification of Polymers: Relevance to Adhesion, Chapter 1. Utrecht: VSP Publishing; 1994.
9. France RM, Short RD. Plasma treatment of polymers: The effects of energy transfer from an argon plasma on the surface chemistry of polystyrene and polypropylene. A high-energy resolution X-ray photoelectron spectroscopy study. Langmuir 1998;14:4827–4835.
10. Li G, Sun Q, Hou X. Graft copolymerization of glycidyl methacrylate onto a polypropylene surface initiated by glow discharge and immobilization of heparin. Acta Polym Sinica 1997;5:589–591.
11. Wang MJ, Chang YI, Poncin-Epaillard F. Acid and basic functionalities of nitrogen and carbon dioxide plasma-treated polystyrene. Surf Interface Anal 2005;37:348–355.
12. Liao JD, Lin SP, Wu YT. Dual properties of the deacetylated ends in chitosan for molecular immobilization and biofunctional effects. Biomacromolecules 2005;6:392–399.
13. Bhat NV, Upadhyay DJ, Dsehmukh RR, Gupta SK. Investigation of plasma-induced photochemical reaction on a polypropylene surface. J Phys Chem B 2003;107:4550–4559.
14. Kou RQ, Xu ZK, Deng HT, Liu ZM, Seta P, Xu Y. Surface modification of microporous polypropylene membranes by plasma-induced graft polymerization of α-allyl glucoside. Langmuir 2003;19:6869–6875.
15. Rasal RM, Janorkar AV, Hirt DE. Poly (lactic acid) modifications. Prog Polym Sci 2010;35:338–356.
16. Linsky CB, Diamond MP, Cunningham T. Adhesion reduction in a rabbit uterine horn model using TC7. J Reprod Med 1987;32:17–20.
17. Jenkins SD, Klamer TW, Parteka JJ, Condon RE. A comparison of prosthetic materials used to repair abdominal wall defects. Surgery 1983;94:392–398.
18. Hooker GD, Taylor BM, Dirman DK. Prevention of adhesion formation with use of sodium hyaluronate-based bioresorbable membrane in a rat model of ventral hernia repair with polypropylene mesh—A randomized controlled study. Surgery 1999;125:211–216.
19. Paragkumar NT, Edith D, Jean-Luc S. Surface characteristics of PLA and PLGA films. Appl Surf Sci 2006;253:2758–2764.
20. Ishaug-Riley SL, Okun LE, Prado G, Applegate MA, Ratcliffe A. Human articular chondrocyte adhesion and proliferation on synthetic biodegradable polymer films. Biomaterials 1999;20:2245–2256.
21. Guo C, Feng L, Zhai J, Wang G, Song Y, Jiang L, Zhu D. Large-area fabrication of a nanostructure-induced hydrophobic surface from a hydrophilic polymer. Chem Phys Chem 2004;5:750–753.
22. Adamson AW, Gast AP. Physical Chemistry of Surfaces, 6th ed. New York: Wiley; 1997. pp 359–360.
23. Shahidzadeh-Ahmadi N, Chehimi MM, Arefi-Khonsari F, Foulon-Belkacemi N, Amouroux J, Delamar M. A physicochemical study of oxygen plasma-modified polypropylene. Colloids Surf A 1995;105:277–289.
24. Yao F, Fua GD, Zhao JP, Kang ET, Neoh KG. Antibacterial effect of surface-functionalized polypropylene hollow fiber membrane from surface-initiated atom transfer radical polymerization. J Membr Sci 2008;319:149–157.
25. Kiss E, Bertoti I, Vargha-Butlerz EI. XPS and wettability characterization of modified poly(lactic acid) and poly(lactic/glycolic acid) films. J Colloid Interface Sci 2002;245:91–98.
26. Elliot MP, Juler GL. Comparison of marlex mesh and microporous teflon sheets when used for hernia repair in the experimental animal. Am J Surg 1979;137:342–344.
27. Ersoy E, Ozturk V, Yazgan A, Ozdoqan M, Gundoqdu H. Effect of polylactic acid film barrier on intra-abdominal adhesion formation. J Surg Res 2008;147:148–152.
28. Hooker GD, Taylor BM, Driman DK. Prevention of adhesion formation with use of sodium hyaluronate-based bioresorbable membrane in a rat model of ventral hernia repair with polypropylene mesh—A randomized, controlled study. Surgery 1999;125:211–216.